This article was downloaded by: [Renmin University of China]
On: 13 October 2013, At: 10:22
Publisher: Taylor & Francis
Informa Ltd Registered in England and Wales Registered Number: 1072954 Registered office: Mortimer House, 37-41 Mortimer Street, London W1T 3JH, UK

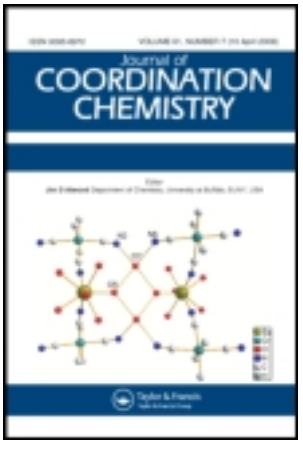

Journal of Coordination Chemistry
Publication details, including instructions for authors and subscription information:
http://www.tandfonline.com/loi/gcoo20

Hydrothermal synthesis and fluorescence of two layered mixed-valence vanadium materials

Xin Liu [a] & Daidi Hu [a]
[a] Department of Chemistry , Capital Normal University , Beijing, 100048, P.R. China
Published online: 11 Jul 2011.

To cite this article: Xin Liu & Daidi Hu (2011) Hydrothermal synthesis and fluorescence of two layered mixed-valence vanadium materials, Journal of Coordination Chemistry, 64:14, 2399-2408, DOI: 10.1080/00958972.2011.598925

To link to this article: http://dx.doi.org/10.1080/00958972.2011.598925

PLEASE SCROLL DOWN FOR ARTICLE

Taylor & Francis makes every effort to ensure the accuracy of all the information (the "Content") contained in the publications on our platform. However, Taylor & Francis, our agents, and our licensors make no representations or warranties whatsoever as to the accuracy, completeness, or suitability for any purpose of the Content. Any opinions and views expressed in this publication are the opinions and views of the authors, and are not the views of or endorsed by Taylor & Francis. The accuracy of the Content should not be relied upon and should be independently verified with primary sources of information. Taylor and Francis shall not be liable for any losses, actions, claims, proceedings, demands, costs, expenses, damages, and other liabilities whatsoever or howsoever caused arising directly or indirectly in connection with, in relation to or arising out of the use of the Content.

This article may be used for research, teaching, and private study purposes. Any substantial or systematic reproduction, redistribution, reselling, loan, sub-licensing, systematic supply, or distribution in any form to anyone is expressly forbidden. Terms & Conditions of access and use can be found at http://www.tandfonline.com/page/terms-and-conditions

Journal of Coordination Chemistry
Vol. 64, No. 14, 20 July 2011, 2399–2408

Taylor & Francis
Taylor & Francis Group

Hydrothermal synthesis and fluorescence of two layered mixed-valence vanadium materials

XIN LIU* and DAIDI HU

Department of Chemistry, Capital Normal University, Beijing, 100048, P.R. China

(*Received 10 August 2010; in final form 6 June 2011*)

Two 2-D layered mixed-valence vanadium materials, $[H_2N(CH_2)_4NH_2]_4[V^{IV}OPO_4V^{V}O(OH)PO_4]_4$ (**1**) and $[H_2N(CH_2)_4NH_2]_2[V_8O_{20}]$ (**2**), have been synthesized under hydrothermal conditions and characterized by infrared spectroscopy, SEM, fluorescence spectroscopy, and single-crystal X-ray diffraction. The layer structure of **1** is composed of $V^{IV}O_6$ octahedra, PO_4 tetrahedra, and $V^{V}O_5$ tetragonal pyramids sharing corners. Compound **2** has a 2-D framework constructed from $[VO_5]$ square pyramids sharing edges and corners. Adjacent $[VO_5]$ layers are connected through the rings to generate a spiral-like inorganic framework with eight-membered ring channels. SEM shows morphology of **1** and **2**. Compounds **1** and **2** show intra-ligand fluorescence emission.

Keywords: Mixed-valence; Layered vanadium materials; Hydrothermal synthesis; Fluorescence

Downloaded by [Renmin University of China] at 10:22 13 October 2013

1. Introduction

Vanadium materials have been the subject of intensive investigation because of their potential applications in catalysis, electrochemistry, sorption, clathration, and ion exchange [1–4]. Examples include vanadium materials with a V/P ratio of 1 : 1 as important catalysts used in the synthesis of maleic anhydride from lighter hydrocarbons [5–7]. An important advance in vanadium chemistry has been the study of the assembly of V–P–O and V–O anions [8, 9] with an inorganic or bridging transition-metal complex into extended frameworks, because of the remarkable features of vanadium surfaces and structural diversity. One of the strategies used for the preparation of vanadium materials is to employ a hydrothermal technique for synthesis. 1-D chain, 2-D layer, and 3-D open-framework structure vanadium materials are prepared in the presence of organic amine and alkali metal cations or metal complexes as structure-directing agents [10–15]; only a few mixed-valence vanadium materials have been reported [16–19].

In this article, we present two vanadium materials, $[H_2N(CH_2)_4NH_2]_4[V^{IV}OPO_4V^{V}O(OH)PO_4]_4$ and $[H_2N(CH_2)_4NH_2]_2[V_8O_{20}]$, which possess 2-D layered networks connected by piperazine dications that are hydrogen bonded to framework oxygens. Both compounds contain mixed-valence vanadium (IV/V) centers. Compound **1** reveals a 2-D framework, constructed from the linkage of phosphate tetrahedra and

*Corresponding author. Email: liuxin661205@yahoo.com.cn

ISSN 0095-8972 print/ISSN 1029-0389 online © 2011 Taylor & Francis
DOI: 10.1080/00958972.2011.598925

vanadyl polyhedra. Compound **2** has a 2-D framework constructed from $[VO_5]$ square pyramids sharing edges and corners. Compounds **1** and **2** show intra-ligand fluorescence.

2. Experimental

2.1. *General procedures*

All starting materials were purchased commercially as reagent grade and used without purification. Infrared (IR) spectra were recorded from 4000 to 400 cm^{-1} on an Alpha Centaurt FT/IR spectrometer with KBr pellets. Field emission scanning electron microscopy (FE-SEM) characterization of the samples was performed on an FEI (HITACHI S-4800) scanning electron micro-analyzer.

Downloaded by [Renmin University of China] at 10:22 13 October 2013

2.2. *Synthesis of compounds*

Compound **1** was synthesized by a mixture of $Zn(NO_3)_2{\cdot}4H_2O$, V_2O_5, piperazine hexahydrate and distilled water with a mole ratio of 1 : 0.5 : 3 : 556. The starting pH was adjusted to 5.0 by addition of 0.3 mL H_3PO_4 and the mixture was stirred for 30 min in air. Then, the reagents were transferred to a Teflon-lined autoclave (20 mL) and kept at 433 K for 4 days. Block gray crystals were isolated after filtering, washing with water, and air-drying. Compound **2** was synthesized by a mixture of $FeCl_3{\cdot}6H_2O$, V_2O_5, piperazine hexahydrate and distilled water (10 mL) with a mole ratio of 1 : 0.5 : 3 : 556. Other conditions were similar to the conditions of **1**. Rod black crystals were isolated after filtering, washing with water, and air-drying.

3. Results and discussion

3.1. *X-ray crystallography*

X-ray single-crystal diffraction reveals that **1** crystallizes in orthorhombic crystal system and the asymmetric unit consists of two crystallographically independent vanadiums. V(1) shows a distorted octahedral geometry (figure 1), coordinated by four phosphate oxygens in the equatorial plane [V(1)–O, 1.956 Å, 1.997 Å, 2.029 Å, 2.079 Å], one vanadyl oxygen [V = O, 1.580 Å] and one phosphate oxygen [V(1)–O(7), 2.419 Å] at axial positions. V(2) displays a distorted square pyramidal geometry. The $V(2)O_5$ has one short bond [V(2) = O(11), 1.596 Å] and four V(2)–O bonds with distances of 1.929–1.964 Å. The O–V(1)–O angles are in the range of 88.64–159.79° and O–V(2)–O of 82.12–151.35°. According to the bond valence sum calculation [20, 21], V(1) and V(2) are +4 and +5. Compound **2** has a $[V_8O_{20}]^{4-}$ layer structure which is linked by piperazine cations. The asymmetric unit of **2** also contains two crystallographically independent vanadiums. There are three types of oxygens: terminal, di-bridging, and tri-bridging. Each V is coordinated by five oxygens while adjacent VO_5 square pyramids connect with each other by sharing edges to make a V–O layer. As shown in figure 2,

Downloaded by [Renmin University of China] at 10:22 13 October 2013

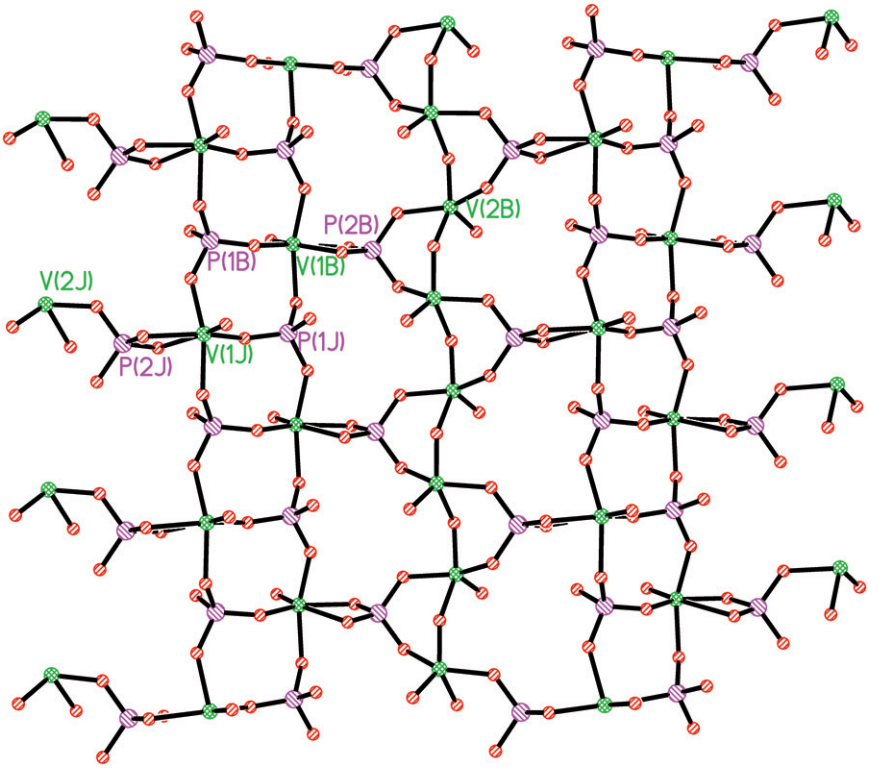

Figure 1. View of the coordination environments of vanadium sites in **1**.

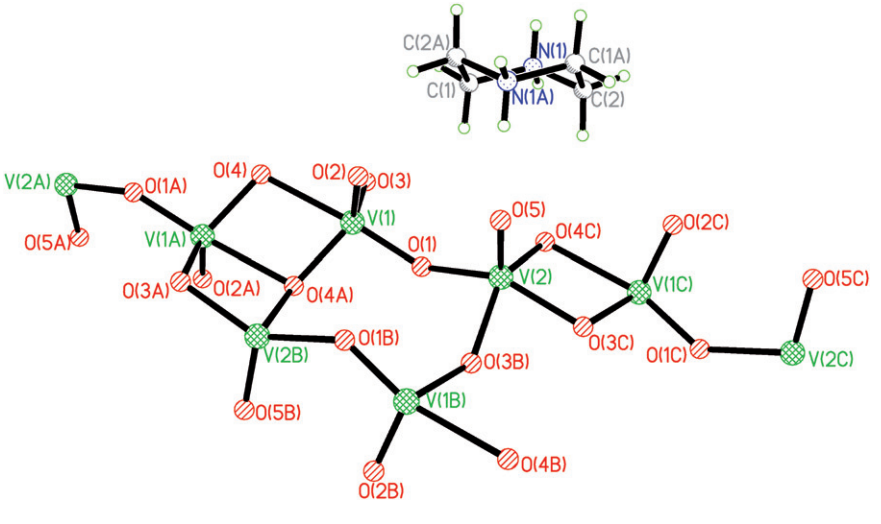

Figure 2. View of the coordination environments of vanadium sites in **2**.

Downloaded by [Renmin University of China] at 10:22 13 October 2013

V(1) shows square pyramidal geometry [V–O, 1.617 Å, 1.729 Å, 1.874 Å, 1.811 Å, 2.270 Å]; $V(2)O_5$ displays a distorted square pyramidal geometry. The $V(2)O_5$ has one short bond [V(2) = O(5), 1.627 Å] and four V(2)–O bonds at 1.915–1.967 Å. Piperazine cations have hydrogen bonding with terminal oxygens from the inorganic framework to template a soft double four-membered ring. According to the bond valence sum calculation [20, 21], V(1) and V(2) are +5 and +4, respectively. The crystallographic data are listed in table 1. Selected bond lengths and angles for **1** and **2** are listed in tables 2 and 3, respectively.

Compounds **1** and **2** have 2-D frameworks linked by piperazines. As shown in figure 3(a), in **1** each $V(1)O_6$ octahedron shares corners with one PO_4 tetrahedron to form the infinite 1-D linear chain along the *c*-axis. Neighboring 1-D chains link to form a ladder. These ladders are linked with corner sharing through adjacent PO_4 tetrahedra and V^VO_5 tetragonal pyramids, forming 2-D layers parallel to the *ac*-plane. There are a number of unusual features associated with this unit in **1**, when compared to reported compounds [5–7, 22]. The vanadium sites are tetragonal pyramids and octahedra rather than tetrahedral or trigonal bipyramidal. Both types of chains are connected by an edge sharing of VO_6 with PO_4 *via* oxygens in a similar way as in $(C_4H_{12}N_2)_2[V_4O_6H(HPO_4)_2(PO_4)_2]$ [22] to form sheets in the *ac*-plane. But **1** is different from $(C_4H_{12}N_2)_2[V_4O_6H(HPO_4)_2(PO_4)_2]$ [22] with the V^VO_5 tetragonal pyramids in the VO_5 chains sharing *trans* corners one by one. The vertices of V^VO_5 tetragonal pyramids are not connected with oxygens from PO_4 tetrahedra. The VO_5 tetragonal pyramids connect with PO_4 tetrahedra to form a Z-like chain. In the $(C_4H_{12}N_2)_2[V_4O_6H(HPO_4)_2(PO_4)_2]$ [22], the VO_5 tetragonal pyramids connect with PO_4 tetrahedra to form an anti Z-like chain. In **1**, 2-D layers stacked along the *b*-axis are linked by bridging

Table 1. The crystallographic data of **1** and **2**.

Empirical formula	$C_4H_{13}N_2O_{11}P_2V_2$ (**1**)	$C_2H_7NO_5V_2$ (**2**)
Formula weight	428.98	226.97
Crystal system	Orthorhombic	Monoclinic
Space group	*Pna*2(1)	*P*2(1)/*n*
Unit cell dimensions (Å, °)		
a	13.135(3)	9.3226(19)
b	15.208(3)	6.5271(13)
c	6.2795(13)	10.260(2)
α	90	90
β	90	106.09(3)
γ	90	90
Volume (Å^3), *Z*	1254.4(4), 4	599.9(2), 4
Calculated density (Mg m^{-3})	2.271	2.513
Absorption coefficient (mm^{-1})	1.808	3.074
F(000)	860	448
Crystal size (mm^3)	0.12 × 0.10 × 0.08	0.14 × 0.10 × 0.10
θ range for data collection (°)	2.05–25.02	3.47–27.72
Limiting indices	$13 \le h \le 15$; $-17 \le k \le 18$; $-7 \le l \le 7$	$-12 \le h \le 11$; $-5 \le k \le 8$; $-12 \le l \le 13$
Reflections collected	7480	3988
Unique reflection	2080 [$R_{int} = 0.0410$]	1392 [$R_{int} = 0.0424$]
Max. and min. transmission	0.8688 and 0.8122	0.7486 and 0.6729
Data/restraints/parameters	2080/15/190	1392/0/91
Goodness-of-fit on F^2	1.087	1.037
Final *R* indices [$I > 2\sigma(I)$]	$R_1 = 0.0290$, $\omega R_2 = 0.0629$	$R_1 = 0.0393$, $\omega R_2 = 0.1113$
R indices (all data)	$R_1 = 0.0310$, $\omega R_2 = 0.0638$	$R_1 = 0.0448$, $\omega R_2 = 0.1133$
Largest difference peak and hole (e Å^{-3})	0.462 and −0.444	1.375 and −0.857

Table 2. Selected bond lengths (Å) and angles (°) for **1**.

V(1)–O(7)	2.419(3)	V(1)–O(5)	1.580(3)
V(1)–O(1)	1.956(3)	V(1)–O(3)#1	1.997(3)
V(1)–O(2)#2	2.029(3)	V(1)–O(6)	2.079(2)
V(2)–O(11)	1.596(3)	V(2)–O(10)#3	1.801(3)
V(2)–O(9)	1.929(3)	V(2)–O(10)	1.950(3)
V(2)–O(8)#3	1.964(3)	O(2)–V(1)#1	2.029(3)
O(3)–V(1)#2	1.997(3)	O(8)–V(2)#4	1.964(3)
O(10)–V(2)#4	1.801(3)	O(5)–V(1)–O(3)#1	100.45(13)
O(5)–V(1)–O(1)	108.36(13)	O(1)–V(1)–O(3)#1	90.64(12)
O(5)–V(1)–O(2)#2	98.93(12)	O(1)–V(1)–O(2)#2	88.64(11)
O(3)#1–V(1)–O(2)#2	159.79(11)	O(5)–V(1)–O(6)	100.81(12)
O(1)–V(1)–O(6)	150.78(11)	O(3)#1–V(1)–O(6)	85.61(11)
O(2)#2–V(1)–O(6)	85.20(11)	O(5)–V(1)–O(7)	166.34(12)
O(1)–V(1)–O(7)	85.25(10)	O(3)#1–V(1)–O(7)	79.87(10)
O(2)#2–V(1)–O(7)	79.94(10)	O(6)–V(1)–O(7)	65.55(9)
O(5)–V(1)–P(2)	133.28(10)	O(1)–V(1)–P(2)	118.35(8)
O(3)#1–V(1)–P(2)	79.77(8)	O(2)#2–V(1)–P(2)	82.82(7)
O(6)–V(1)–P(2)	32.51(7)	O(7)–V(1)–P(2)	33.11(6)
O(11)–V(2)–O(10)#3	105.74(15)	O(11)–V(2)–O(9)	106.79(15)
O(10)#3–V(2)–O(9)	87.03(12)	O(11)–V(2)–O(10)	102.77(15)
O(10)#3–V(2)–O(10)	151.35(9)	O(9)–V(2)–O(10)	82.12(12)
O(11)–V(2)–O(8)#3	105.54(14)	O(10)#3–V(2)–O(8)#3	90.19(12)
O(9)–V(2)–O(8)#3	147.07(14)	O(10)–V(2)–O(8)#3	84.87(12)

Symmetry transformations used to generate equivalent atoms: #1, $-x$, $-y+1$, $z-1/2$; #2, $-x$, $-y+1$, $z+1/2$; #3, $-x+1$, $-y+1$, $z-1/2$; #4, $-x+1$, $-y+1$, $z+1/2$.

Table 3. Selected bond lengths (Å) and angles (°) for **2**.

V(1)–O(2)	1.617(2)	V(1)–O(1)	1.729(2)
V(1)–O(4)#1	1.809(2)	V(1)–O(3)	1.873(2)
V(1)–O(4)	2.269(3)	V(2)–O(5)	1.627(2)
V(2)–O(4)#2	1.915(2)	V(2)–O(1)	1.922(2)
V(2)–O(3)#3	1.955(2)	V(2)–O(3)#2	1.967(3)
V(2)–V(2)#4	3.0585(13)	O(3)–V(2)#5	1.955(2)
O(3)–V(2)#6	1.967(3)	O(4)–V(1)#1	1.809(2)
O(2)–V(1)–O(1)	104.82(12)	O(2)–V(1)–O(4)#1	113.17(12)
O(1)–V(1)–O(4)#1	100.31(11)	O(2)–V(1)–O(3)	114.31(12)
O(1)–V(1)–O(3)	96.65(10)	O(4)#1–V(1)–O(3)	122.80(11)
O(2)–V(1)–O(4)	89.94(11)	O(1)–V(1)–O(4)	164.78(10)
O(4)#1–V(1)–O(4)	76.63(11)	O(3)–V(1)–O(4)	73.42(9)
O(5)–V(2)–O(4)#2	107.53(11)	O(5)–V(2)–O(1)	105.83(11)
O(4)#2–V(2)–O(1)	90.63(10)	O(5)–V(2)–O(3)#3	110.75(11)
O(4)#2–V(2)–O(3)#3	139.94(11)	O(1)–V(2)–O(3)#3	90.06(10)
O(5)–V(2)–O(3)#2	107.85(11)	O(4)#2–V(2)–O(3)#2	80.05(10)
O(1)–V(2)–O(3)#2	146.32(11)	O(3)#3–V(2)–O(3)#2	77.48(10)

Symmetry transformations used to generate equivalent atoms: #1, $-x+1$, $-y$, $-z+2$; #2, $x-1/2$, $-y+1/2$, $z-1/2$; #3, $-x+1/2$, $y-1/2$, $-z+3/2$; #4, $-x$, $-y$, $-z+1$; #5, $-x+1/2$, $y+1/2$, $-z+3/2$; #6, $x+1/2$, $-y+1/2$, $z+1/2$.

piperazines to further extend the structure to a 3-D framework. There are many channels in **1**. The channels comprise four vanadium cores and three phosphorus cores are 7-membered. Pores comprising tetranuclear cores along the *b*-axis are shown in figure 3(a). Free diprotonated piperazines are located in these channels along the *b*-axis. The layers are bonded to the piperazine cations through H-bonds with N···O in the range 2.668–3.299 Å.

The layers in **2** are constructed from [VO_5] square pyramids sharing edges and corners, as shown in figure 3(b), similar to those found in pure V_2O_5 [23].

Downloaded by [Renmin University of China] at 10:22 13 October 2013

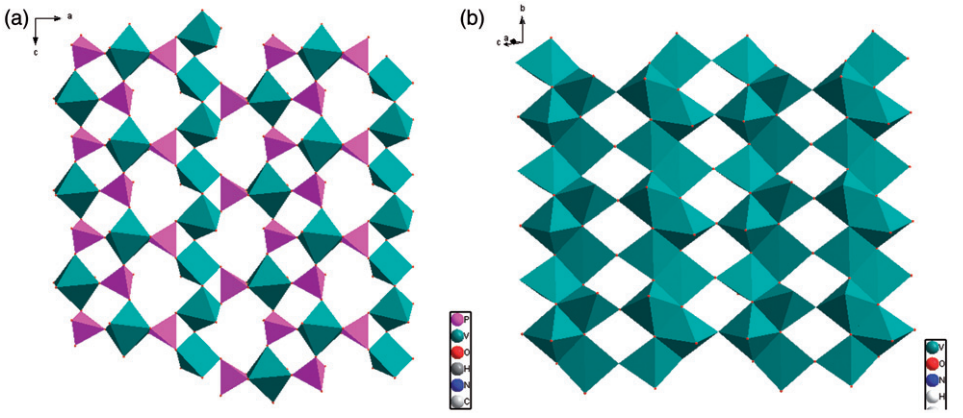

Figure 3. (a) Polyhedra of layer structure of **1** viewed from the crystallographic *b*-axis and (b) Polyhedra of $[VO_5]$ layer structure of **2** projected from the *a*-axis.

However, unlike the neutral vanadium oxide layers in V_2O_5 which contain only fully oxidized vanadium(V) centers, the vanadium oxide layers in **2** contain mixed-valence vanadium (IV/V) centers, conferring a formal negative charge to these layers. The interleaved layers, which are composed of $[H_2N(CH_2)_4NH_2]_4^{2+}$ chains, have a formal positive charge. The framework structure can alternatively be viewed as composed of reduced and negatively charged layers of $[V_2O_5]^-$ intercalating $[H_2N(CH_2)_4NH_2]_4^{2+}$ layers and held together by host–guest interactions [24, 25]. Adjacent $[VO_5]$ layers are connected through sharing corners to generate a spiral-like inorganic framework with eight-membered ring channels along the *a*-axis. The layers are bonded to the piperazine cations through H-bonds with N···O in the range 2.836–2.965 Å.

3.2. *Effects of synthesis conditions on the crystallization of 1 and 2*

Reaction conditions strongly affect the final crystal phase, size, and morphology for vanadium materials. Herein, a series of experiments are performed to investigate the effects of reaction temperature, reaction time, metal salts, and pH on crystallization. The impact of reaction conditions on **1** are listed in table 4. When the reaction temperature in the synthesis of **1** is below 433 K, gray solutions are obtained. The optimum reaction temperature is 433 K. When the reaction time is from 4 days to 2 days, small gray crystals of **1** are obtained. As shown in table 4, the addition of $Zn(NO_3)_2{\cdot}4H_2O$ can accelerate formation of **1** and shorten the crystallization time from 7 to 4 days. In the synthesis of **1**, H_3PO_4 acts as a structure-directing agent and also as an acid to adjust the pH of the aqueous solution. When pH of the solution is more than 6 or less than 4, no crystals are obtained. That may be because $Zn(NO_3)_2$ is transformed into $Zn(OH)_2$ in alkaline conditions. Thus, there is an optimum pH = 5 for the crystallization of **1**. The impact of reaction conditions on **2** are listed in table 5. When reaction temperature is below 433 K in the synthesis of **2**, black solutions or powders are obtained. The optimum reaction temperature of **2** is also 433 K. In the synthesis of **2**, the addition of $FeCl_3{\cdot}6H_2O$ accelerates the formation of **2**, shortening the crystallization time from 6 to 4 days. As shown in table 5, pH of the reaction solution is 8. If pH of the solution is less than 8,

Downloaded by [Renmin University of China] at 10:22 13 October 2013

Table 4. The impact of reaction conditions on **1**.

Temperature (K)	Time (days)	pH	Metal salts	Products
393	4	5	$Zn(NO_3)_2 \cdot 4H_2O$	Gray solution
413	4	5	$Zn(NO_3)_2 \cdot 4H_2O$	Dark gray solution
433	2	5	$Zn(NO_3)_2 \cdot 4H_2O$	Small gray crystals (compound **1**)
433	4	5	$Zn(NO_3)_2 \cdot 4H_2O$	Block gray crystals (compound **1**)
433	4	5	No metal salts	Dark gray solution
433	7	5	No metal salts	Small gray crystals (compound **1**)
433	4	8	$Zn(NO_3)_2 \cdot 4H_2O$	Solid powder and colorless solution
433	4	7	$Zn(NO_3)_2 \cdot 4H_2O$	Solid powder and colorless solution
433	4	6	$Zn(NO_3)_2 \cdot 4H_2O$	Gray solution
433	4	4	$Zn(NO_3)_2 \cdot 4H_2O$	Small gray crystals (compound **1**)

The mole ratio of $V_2O_5/Zn(NO_3)_2 \cdot 4H_2O/C_4H_{10}N_2 \cdot 6H_2O/H_2O$ is 0.5 : 1 : 3 : 556. H_3PO_4 acts as an acid to adjust the pH of the aqueous solution.

Table 5. The impact of reaction conditions on **2**.

Temperature (K)	Time (days)	pH	Metal salts	Products
393	4	8	$FeCl_3 \cdot 6H_2O$	Black solution
413	4	8	$FeCl_3 \cdot 6H_2O$	Solid powder and black solution
433	2	8	$FeCl_3 \cdot 6H_2O$	Small black crystals (compound **2**)
433	4	8	$FeCl_3 \cdot 6H_2O$	Rod black crystals (compound **2**)
433	4	8	No metal salts	Black solution
433	6	8	No metal salts	Small black crystals (compound **2**)
433	4	7	$FeCl_3 \cdot 6H_2O$	Black solution

The mole ratio of $V_2O_5/FeCl_3 \cdot 6H_2O/C_4H_{10}N_2 \cdot 6H_2O/H_2O$ is 0.5 : 1 : 3 : 556.

no crystals are obtained. Piperazines act not only as templating agent but also as organic base to affect the pH of the aqueous solution.

3.3. *IR spectroscopy*

In IR spectra, characteristic vibration modes of **1** are observed for ν(P–O) at 1082 cm^{-1}, 1066 cm^{-1}, ν(V = O) at 980 cm^{-1}, 951 cm^{-1}. The characteristic absorption bands of piperazine occur at 1634 cm^{-1}, 1592 cm^{-1}, 1460 cm^{-1}, and 1382 cm^{-1}. The characteristic vibration modes of **2** are observed for ν(V–O) at 947 cm^{-1}. The characteristic absorption bands of piperazine occur at 1553 cm^{-1}, 1419 cm^{-1}, and 1384 cm^{-1}.

3.4. *SEM*

Figure 4 shows FE-SEM images of **1** and **2**. Morphology of **1** (figure 4a) is not a regular array and the surface of **1** is not smooth. Obviously, **2** (figure 4b) is a homogeneous phase with uniform particles. Compound **2** shows large quantities of rod-like crystallites with lengths of several micrometers.

Downloaded by [Renmin University of China] at 10:22 13 October 2013

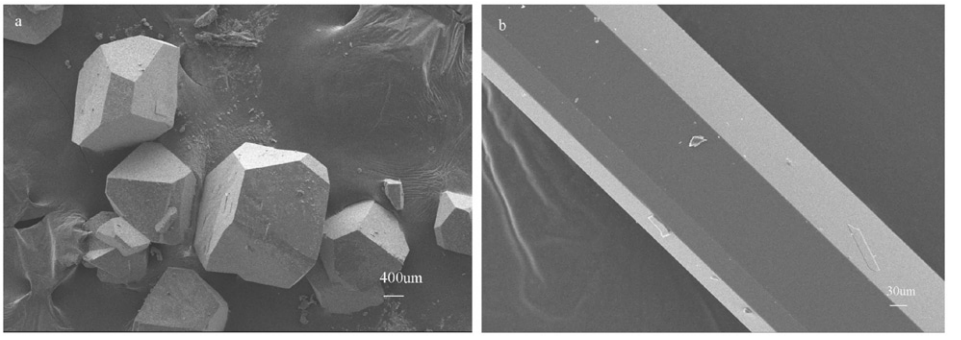

Figure 4. SEM images of **1** (a) and **2** (b).

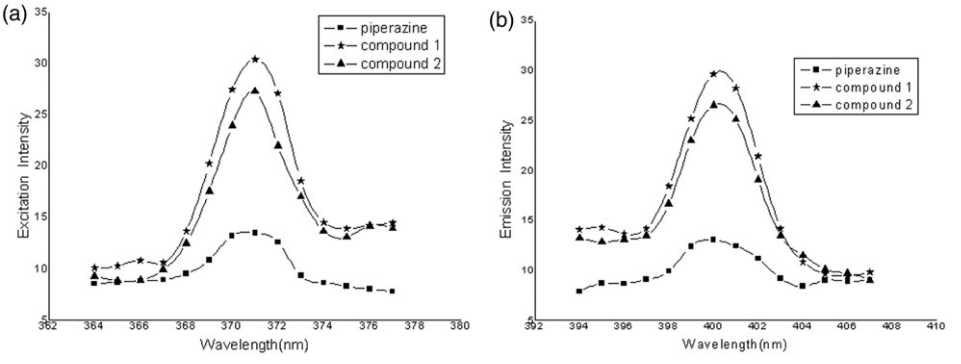

Figure 5. (a) Excitation fluorescence of piperazine, **1** and **2** and (b) emission fluorescence of piperazine, **1** and **2**.

3.5. *Fluorescence spectroscopy*

1, **2**, and piperazine fluoresce in the solid state. As shown in figure 5(a), the strongest excitation peaks for **1**, **2**, and piperazine are similar at 371 nm. As displayed in figure 5(b), the emission spectra of **1** and **2** exhibit a main peak at 400 nm excited at 371 nm, assigned to intra-ligand fluorescent emission.

4. Conclusion

Two 2-D layered mixed-valence vanadium materials, $[H_2N(CH_2)_4NH_2]_4[V^{IV}OPO_4V^{V}O(OH)PO_4]_4$ and $[H_2N(CH_2)_4NH_2]_2[V_8O_{20}]$, have been synthesized by hydrothermal methods. Block gray **1** are obtained in acidic conditions while rod black **2** are obtained in alkaline conditions. Piperazines act not only as template agent but also as organic base to affect the pH of the aqueous solution. There are mixed-valence vanadium (IV/V) centers in **1** and **2**. Compound **1** has a 2-D framework from linkage of

Downloaded by [Renmin University of China] at 10:22 13 October 2013

phosphate tetrahedra and vanadyl polyhedra. The crystal structure of **1** contains PO_4 tetrahedra, VO_5 tetragonal pyramids, and VO_6 octahedra, where corner-sharing linkage between VO_5 tetragonal pyramids, VO_6 octahedra, and PO_4 tetrahedra are crucial in the formation of the 2-D frameworks. The structure of **1** reflects the variability of vanadium coordination numbers, as well as the diverse connectivity patterns which may be generated between a given vanadium polyhedral type and the various phosphate tetrahedra present. Compound **2** has a 2-D framework constructed from $[VO_5]$ square pyramids sharing edges and corners. The framework structure of **2** can be viewed as composed of reduced and negatively charged layers of $[V_2O_5]^-$ intercalating $[H_2N(CH_2)_4NH_2]_4^{2+}$ layers and held together by host–guest interactions. The organic diprotonated piperazine cations interact with oxygens in the inorganic network through hydrogen bonds. Compounds **1** and **2** in the solid state show intra-ligand fluorescence emission. This work enriches the library of vanadium materials.

Downloaded by [Renmin University of China] at 10:22 13 October 2013

Supplementary material

The CCDC numbers of $[H_2N(CH_2)_4NH_2]_4[V^{IV}OPO_4V^{V}O(OH)PO_4]_4$ (**1**) and $[H_2N(CH_2)_4NH_2]_2[V_8O_{20}]$ (**2**) are 682488 and 681598. The data acquisition of these materials are available free of charge *via* the Internet at http://www.ccdc.cam.ac.uk/deposit.

Acknowledgments

This work was supported by Scientific Research common program of Beijing Municipal Commission of Education (KM200510028005).

References

[1] D.W. Murphy, P.A. Christian. *Science*, **205**, 651 (1979).
[2] Y.P. Zhang, R.C. Haushalter, A. Clearfield. *Inorg. Chem.*, **35**, 4950 (1996).
[3] D. Lemordant, A. Bouhaouss, P. Aldebert, N. Baffier. *Mater. Res. Bull.*, **21**, 273 (1986).
[4] A. Bouhaouss, P. Aldebert. *Mater. Res. Bull.*, **18**, 1247 (1983).
[5] B.K. Hodnett. *Catal. Rev. Sci. Eng.*, **27**, 373 (1985).
[6] G. Centi, F. Trifiro, J.R. Ebner, V.M. Franchetti. *Chem. Rev.*, **88**, 55 (1988).
[7] E. Bordes, P. Courtine. *J. Catal.*, **57**, 236 (1979).
[8] M.J. Cheng, K. Chenoweth, J. Oxgaard. *J. Phys. Chem. C*, **111**, 5115 (2007).
[9] M.I. Khan, E. Yohannes, V.O. Golub. *Chem. Mater.*, **19**, 4890 (2007).
[10] J. Do, R.P. Bontchev, A.J. Jacobson. *J. Solid State Chem.*, **154**, 514 (2000).
[11] P.J. Hagrman, J. Zubieta. *Inorg. Chem.*, **40**, 2800 (2001).
[12] R.N. Devi, J. Zubieta. *Inorg. Chim. Acta*, **338**, 165 (2002).
[13] W. Ouellette, E. Burkholder, J. Zubieta. *Solid State Sci.*, **6**, 77 (2004).
[14] V. Soghomonian, R.C. Haushalter, Q. Chen, J. Zubieta. *Inorg. Chem.*, **33**, 1700 (1994).
[15] V. Soghomonian, R.C. Haushalter, J. Zubieta, C.J. O'Connor. *Inorg. Chem.*, **35**, 2826 (1996).
[16] C.M. Liu, S. Gao, H.Z. Kou. *Chem. Commun.*, 1670 (2001).
[17] Z. Shi, L.R. Zhang, G.S. Zhu, G.Y. Yang, J. Hua, S.H. Feng. *Chem. Mater.*, **11**, 3565 (1999).
[18] Y.P. Zhang, R.C. Haushalter, A. Clearfield, J. Zubieta. *Angew. Chem., Int. Ed.*, **35**, 989 (1996).
[19] G.H. Huan, J.W. Johnson, A.J. Jacobson, J.S. Merola. *J. Solid State Chem.*, **91**, 385 (1991).

[20] S. Boudin, A. Guesdon, A. Leclaire, M.M. Borel. *Int. J. Inorg. Mater.*, **2**, 561 (2000).
[21] I.D. Brown, K.K. Wu. *Acta Crystallogr.*, **B32**, 1957 (1976).
[22] V. Zima, K.H. Lii. *J. Solid State Chem.*, **172**, 424 (2003).
[23] R. Enjalbert, J. Gally. *Acta Crystallogr.*, **C42**, 1467 (1986).
[24] Y.K. Shan, R.H. Huang, S.D. Huang. *Angew. Chem., Int. Ed.*, **38**, 1751 (1999).
[25] M.G. Kanatzidis, C.G. Wu. *J. Am. Chem. Soc.*, **111**, 4139 (1989).

Downloaded by [Renmin University of China] at 10:22 13 October 2013